

Evaluation of EUV resist performance below 20-nm CD using helium ion lithography

Diederik Maas^{*a}, Emile van Veldhoven^a, Anja van Langen–Suurling^b, Paul F.A. Alkemade^b, Sander Wuister^c, Rik Hoefnagels^c, Coen Verspaget^c, Jeroen Meessen^c and Timon Fliervoet^c
^aTNO, Stieltjesweg 1, Delft, The Netherlands; ^bKavli Institute of Nanoscience, Delft University of Technology, Lorentzweg 1, Delft, The Netherlands; ^cASML, De Run 6665, Veldhoven, The Netherlands

ABSTRACT

For the introduction of EUV lithography, development of high performance EUV resists is of key importance. This development involves studies into resist sensitivity, resolving power and pattern uniformity. We have used a sub-nanometer-sized 30 keV helium ion beam to expose chemically amplified (CAR) EUV resists. There are similarities in the response of resists to He⁺ ions and EUV photons: both excite Secondary Electrons with similar energy distributions. The weak backscattering of the He⁺ ions results in ultra-low proximity effects. This fact enables the exposure of dense and detailed patterns by focused He⁺ ion beams without the need for proximity correction. This paper presents contact holes and lines at 40-nm pitch in an EUV CAR resist. We have used resist sensitivity, contrast, resolution (CD) and pattern fidelity (LCDU, LWR and dose-to-print) as metrics for a comparison of SHIBL with EUVL. We show that Scanning Helium Ion Beam Lithography (SHIBL) can be a useful and economically attractive technology to (pre-)screen novel EUV resists prior to their final performance evaluation in an EUV scanner.

Keywords: Lithography, EUV lithography, Scanning Helium Ion Beam Lithography, EUV resist characterization, Helium Ion Microscope, Proximity effect, Energy transfer

1. INTRODUCTION

For the introduction of EUV lithography, development of high performance EUV resists is of key importance. This development involves studies into sensitivity, resolving power and pattern uniformity [1-3]. We have used a sub-nanometer-sized 30 keV helium ion beam to expose chemically amplified (CAR) EUV resists. As is shown in Figure 1 the shape of the large area dose-response curve is highly similar for EUV and 30 keV helium ion exposure. Yet there is a large difference in the required number of primary particles: we have observed that a single 30 keV helium ion is as effective as 150 EUV photons. This is attributed mainly to the fact that an EUV photon interacts only once (or not at all) with the resist, whereas a helium ion scatters inelastically many times while traversing the resist, and often releases one or more SEs in each collision.

The absence of proximity effects is a clear advantage of SHIBL over Electron Beam Lithography (EBL) [4-6], although today EBL is often used to pre-screen EUV resist [7]. EUV interference lithography is another tool in resist resolution and sensitivity studies [8]. SHIBL potentially complements this technology by offering a more flexible pattern design, enabling the study of corners, edges, elbows and contact holes and even arbitrary patterns that might occur in chip designs [9].

This paper presents exposures of contact holes and lines-and-spaces with a Critical Dimension (CD) of 8 – 30 nm at 40 nm pitch in a state-of-the-art chemically amplified EUV resist of type A using 30 keV He⁺ ions. We compare these results with EUV Lithography (EUVL) exposures performed with ASML's NXE: 3300B scanner on a similar CAR resist of type B. We use resist sensitivity, contrast, resolution (CD) and pattern fidelity (LCDU, LWR and dose-to-print) as metrics for a comparison of SHIBL with EUVL.

We show that SHIBL can be a useful and economically attractive technology to pre-screen novel EUV resists prior to their final performance evaluation in an EUV scanner.

*diederik.maas@tno.nl; phone +31 888 666 524; www.tno.nl

2. RESIST ACTIVATION

2.1. Exposure of fine and dense patterns on EUV resists

Besides some differences, there are remarkable similarities in the response of resists to He^+ ions and EUV photons. Both types of primary particle beams traverse the resist while interacting with the resist and substrate atoms. The weak scattering of the He^+ ions results in ultra-low proximity effects, which is similar to EUV exposures. As a result, for either primary beam type, the projection of the desired exposure pattern is relatively easily achieved without complex compensation for proximity effects, e.g. by computational lithography and the like. A principal difference is that for EUVL the pattern is projected on the resist using a patterned mask, whereas in Scanning Helium Ion Beam Lithography (SHIBL) electrostatic beam deflection is used to scan the beam over the resist, an approach that is many orders of magnitude slower. The serial approach of SHIBL prohibits high-volume production. Yet, this is not critical when exposing relatively small areas, e.g. to investigate fundamental properties of a resist like sensitivity, resolution and line width roughness). Finally, the large depth-of-field of the helium beam (given the beam angle of typically less than 1 mrad) supports well-focused projection of the pattern on the resist [10].

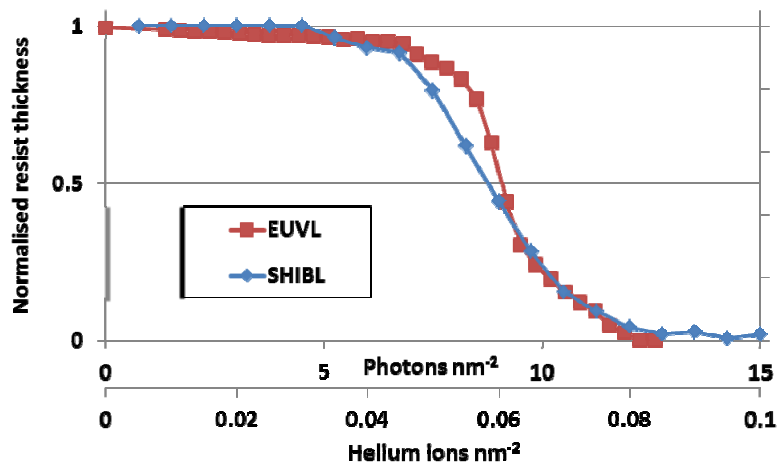


Figure 1 Large-area dose-response curves for EUV CAR resist A exposed to EUV and 30-keV He^+ . The EUV dose-to-clear is $12.8 \text{ photons nm}^{-2}$, i.e. 18 mJ cm^{-2} , the contrast is 3. The He^+ ion dose-to-clear is $0.085 \text{ ions nm}^{-2}$, which is equal to 1.36 uC cm^{-2} or 41 mJ cm^{-2} , the contrast is 2. He^+ ions are approximately 150 more effective than EUV photons.

2.2. Resist activation

To provide some insight in the (dis)similarities between EUV and helium ion exposure, we will briefly summarize the cascade of events when a primary particle interacts with the resist. According to Kozawa [11], EUVL is different from classical optical lithography in the sense that the resist activation starts with core-shell ionization of a resist atom. The generated Secondary Electron (SE) travels some distance until it is captured by an acid generator, which in turn dissociates into a mobile H^+ ion and an immobile anion. When comparing the SE generating processes for He^+ and EUV it can be noted that the respective energy spectra are remarkably alike:

- Typically, the absorption of an EUV photon generates a high-energy electron that relaxes by the excitation of Secondary Electrons (SEs). An EUV photon carries $\sim 92 \text{ eV}$ of energy. Absorption by a target atom releases a high-energy core electron with a kinetic energy between $60\text{--}75 \text{ eV}$. This electron diffuses a few nanometer and creates typically 2-8 SEs, each with an energy of $6\text{--}9 \text{ eV}$. A significant fraction of these SEs activates acidic resist molecules [11, 12].
- Fast, light ions in matter lose their energy mainly by electronic excitations and ionizations. As a consequence, a beam of 30-keV He^+ ions produces many SEs, most of them with energies less than 10 eV [13].

After the interaction with a resist atom, the EUV photon is gone, whereas the He^+ ion continues its way through the resist in almost the same direction, but at a slightly lower energy.

Figure 1 shows the large-area dose-response curve for 92-eV EUV and 30-keV He^+ ion exposures. The shapes of the curves are similar, suggesting a similar resist activation mechanism. The dose-to-clear for EUV CAR A is $12.8 \text{ EUV photons nm}^{-2}$ and $0.085 \text{ He}^+ \text{ nm}^{-2}$ respectively. Hence, 150 times less ions than EUV photons are needed for the same resist modification.

2.3. Amount of SEs released in the resist per EUV photon and per He⁺ ion

Kozawa and Tagawa [11] attribute an important role to SEs in the resist exposure mechanism. Here we estimate for our experiment the number of SEs generated in the resist layer per photon and per 30-keV He⁺ ion. First the EUV CAR resist A is analyzed by X-ray photoelectron spectrometry (XPS). The recorded XPS spectrum was analyzed with respect to the actual resist composition, assuming 1.5 hydrogen atoms per carbon atom. The SE generation is quantified using the interactions of EUV photons and 30-keV He⁺ ions with the resist.

An EUV CAR resist layer of 40 nm absorbs approximately 15% of the 92-eV EUV photons [14]. The dissipated energy density at dose-to-clear is calculated to be approximately 180 eV nm⁻². The average SE yield per absorbed EUV photon is still a topic of debate [12,15]. Reported values lie between 2 and 8, on average corresponding to the release of 0.15 x 12.8 x ~4 ≈ 8 SEs nm⁻² at dose-to-clear.

Figure 2 shows the energy loss of 30 keV He⁺ ions by ionizations as computed using SRIM [16]. The average loss per ion in the 40-nm thick EUV CAR resist layer is 3.6 keV, predominantly by ionizations. Assuming an average SE energy of 10 eV¹[13], each He⁺ ion generates approximately 360 secondary electrons in the resist. At 0.085 He⁺ ions nm⁻², the average ionization energy is thus 306 eV nm⁻². This corresponds to ~30 SEs nm⁻² at dose-to-clear. Similar numbers for generated SEs from He⁺ ions are reported earlier [6], and studied in more detailed by Monte Carlo modeling [17].

Recently, Monte Carlo modeling by Torok et al. [12] showed that the efficacy of resist activation depends strongly on the *specific* energy of a low-energy electron. The factor of 4 discrepancy in the estimated number of involved SEs between SHIBL and EUVL is regarded to be within the uncertainty. In conclusion, it is stated that the resist is activated by the low-energy SEs and not by the 30-keV He⁺ ions directly. Therefore, we postulate that SHIBL and EUVL record similar resist exposure processes.

Target Ionization

Total Ionization = 26.7 keV / Ion

Total Phonons = 2.9 keV / Ion

Total Target Damage = 0.31 keV / Ion

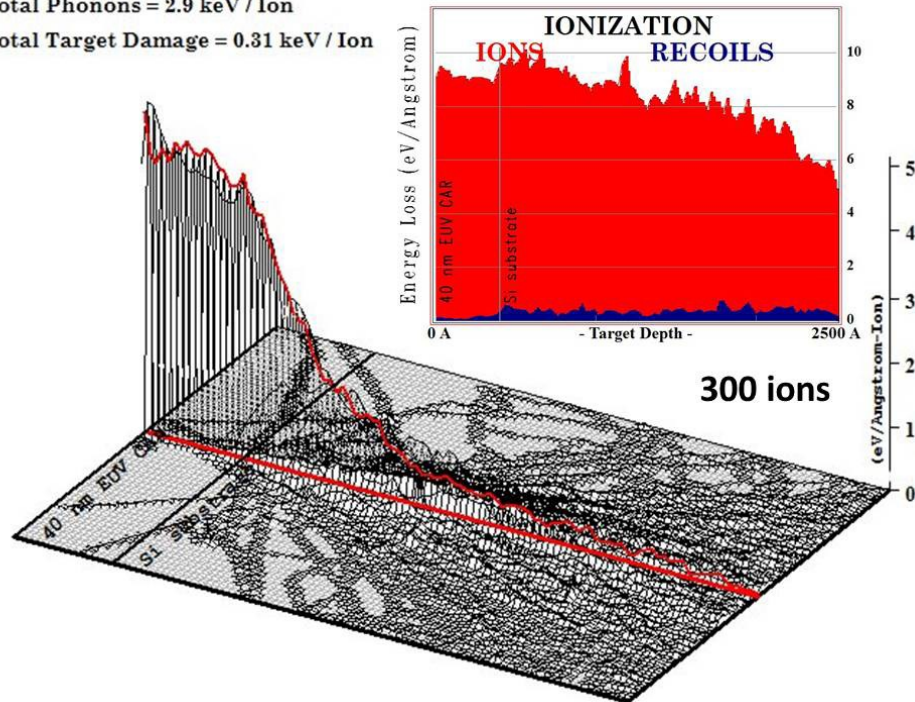


Figure 2 Ionization in the resist as computed by SRIM, for 30-keV He⁺ ions. The inset shows the energy loss through ionization (red) and recoil (blue) as a function of depth.

¹ Petrov and Vyvenko [13] have reported an average SE energy of 6eV measured in the vacuum. As the SE has overcome the work function of the target material, which typically is 4eV, we conclude that the SEs in the resist have on average ~10 eV kinetic energy.

3. EXPERIMENTAL

A 40-nm thick EUV CAR resist of type A was spin-coated on a Si wafer. The Si wafer was coated with a monolayer of HMDS as a primer to prevent resist delamination during development.

The EUV CAR A SHIBL exposures were performed on a Zeiss Orion Plus™ Helium Ion Microscope (HIM) at the TNO Van Leeuwenhoek Laboratory (VLL) in Delft. The HIM was set to 30-keV beam energy. The beam was focused at a working distance of 7 mm with the 5- μm beam-limiting aperture. The resulting beam angle spread is less than 1 mrad, yielding a probe size d_{50} of 0.7 nm and a depth-of-field larger than 0.5 μm [10]. A pattern generator (Raith Elphy MultiBeam) was used for the beam blanking and scanning. The beam current was set to 0.10 pA \pm 0.02 pA (1-sigma)².

Point, or contact hole, exposures in arrays of 24x24 at a pitch of 40 nm were made. The exposure time of the arrays was varied exponentially in steps of 20% from 100 μs to 500 μs per point. Additionally, lines-and-spaces (24 lines at 40-nm, 50-nm, and 60-nm pitch) and large boxes (10 μm by 25 μm) were made in the range of 0.1 to 1 $\mu\text{C cm}^{-2}$. The exposure dose was varied by adjusting the pixel dwell time. The trenches are written as a single-pixel wide line at 2-nm step size. The beam step size for the large boxes was also 2 nm. The box exposures were used to determine the dose-response curve.

The Normalized Image Log Slope (NILS) for the exposed patterns and SHIBL was estimated to exceed 10, indicative of easy imaging of the pattern on the resist [18].

The EUV CAR resist of type B exposures were performed on an ASML NXE: 3300B, using a Quasar 30 illumination setting for the contact holes.

The standard CAR resist post-exposure bake (PEB) and the ASML Process Of Record (POR) development recipe have been applied. There were some differences in the development recipes used at ASML in Veldhoven and at the VLL in Delft. In the VLL, the post-exposure bake of EUV CAR resist of type A took place at 110 degrees Celsius for 1 minute on a hot plate (Stuart Digital SD300). At ASML, the EUV CAR of resist type B was processed at a Tokyo Electron (TEL) wafer track using a development recipe generated by TEL. This consists of generating a puddle while the wafer is stationary and a rinse while the wafer is rotating, optimized for uniformity. In case of the contact hole exposures and the contrast curve exposures, a DIW rinse was used, whereas for the lines-and-spaces a surfactenated rinse was used. This rinse was optimized to reduce pattern collapse of the resist material.

The box exposures were inspected with a Bruker Dektak NXT profilometer.

The contact holes and lines-and-spaces were measured with a Hitachi CD SEM CG-4000, operating at 500-eV beam energy. The CD of the contact holes and of the lines were obtained from the CD SEM images using the software (SW) package Terminal PC V8 (Hitachi) with a 50% threshold algorithm.

4. SHIBL EXPOSURES OF HIGH RESOLUTION PATTERNS

4.1. Dense Contact Holes at 40-nm pitch – exposed with SHIBL and EUVL

Figure 3 shows CD SEM images of three dense arrays of point exposure, made in EUV CAR resist of type A using SHIBL (panel a-c) and in EUV CAR resist of type B using EUVL (panel e). It can be observed that the point exposures resulted in circular holes, mimicking the dense array pattern for contact holes. The ion dose ranged from 60 – 260 ions per hole (in 9 steps with a dose-multiplication factor of 1.2). The measured contact hole CD is used to convert the dose-per-hole to a dose-per-hole-area³, yielding 0.62 – 1.17 ion nm^{-2} or 10 – 19 $\mu\text{C cm}^{-2}$. The results of the CD analysis are shown in panel d. The average CD ranges from 12.5 to 19.2 nm, whereas the EUVL contact hole CD is 20.2 nm. Ergo, with SHIBL we did not reach a 1:1 pitch. At the largest doses, larger fractions of the contact holes were observed to be too distorted for automated analysis. The SHIBL LCDU increases with dose from 2.7 to 10 nm (3 σ), whereas the EUVL LCDU is 2.9 nm (3 σ). The percentage of CHs that meet the criteria of the CD evaluation software ranges from 16% to 100%. Only for doses between 100-180 ions per CH the 95% threshold for a reliable CD measurement is met. Hence, LCDU values outside this dose range are not regarded as reliable.

²Note that measurements of such low beam currents are not very accurate. But since the beam current is proportional to the helium partial pressure in the ion source section [10], we measured the current at a tenfold increased pressure of 10⁻⁵ mbar.

³Note that the hole area is not proportional to the ion dose-per-hole.

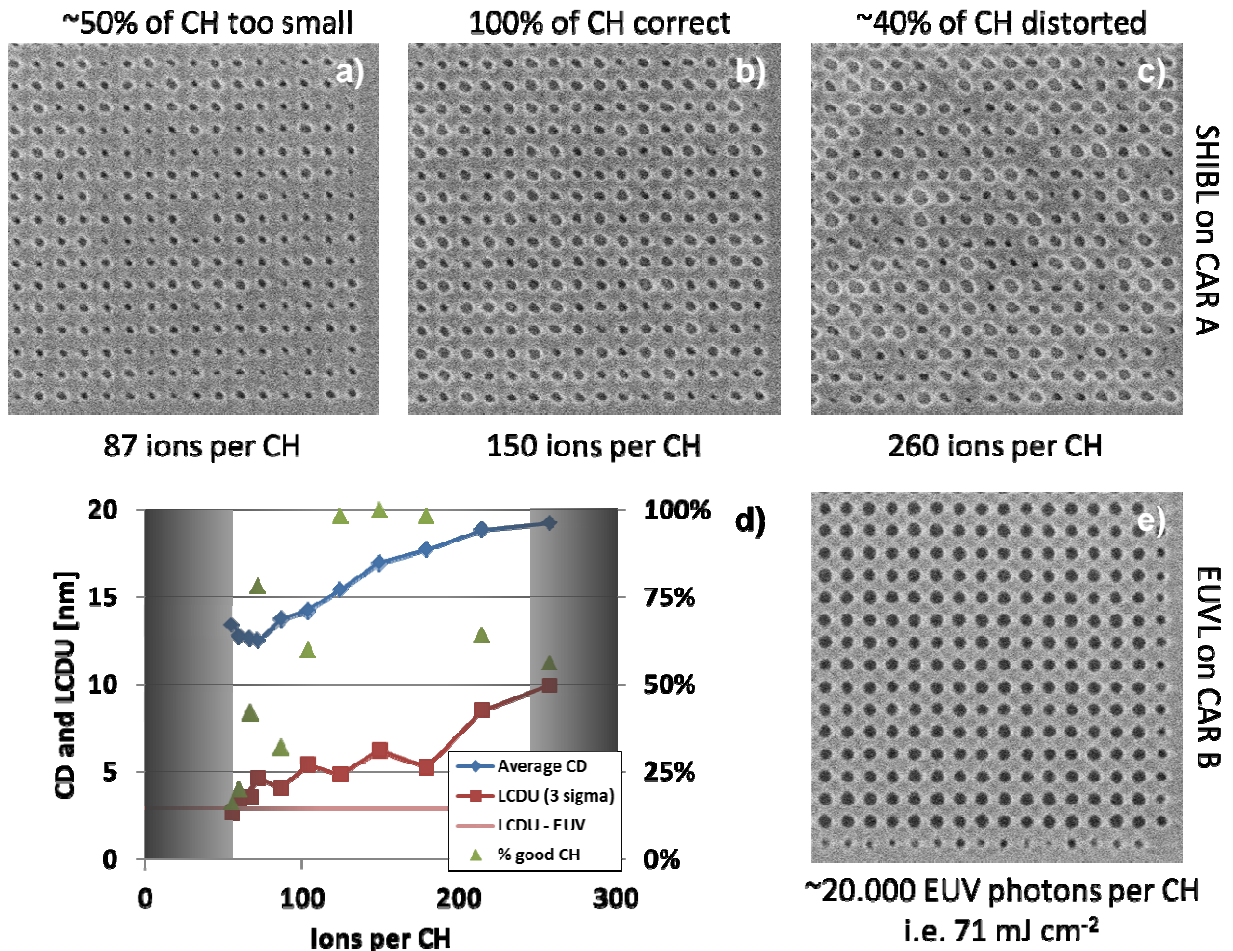


Figure 3 a-c: CD SEM images of arrays of contact holes at 40-nm pitch in EUV CAR resist of type A exposed with SHIBL at three different doses. Panel d shows the CD, LCDU and the fraction of contact holes that qualified for size analysis. Panel e shows an EUVL exposure of a similar array of contact holes at EUV CAR resist of type B, exposed at 5.3 times the dose-to-clear of 13.5 mJ cm⁻². The contact holes in the outer rows are smaller due to proximity or interference effects.

4.2. Dense lines-and-spaces made with SHIBL and EUVL

Similarly to the contact holes, we have exposed EUV CAR resist of type A with dense lines-and-spaces patterns using SHIBL at a dose range between 2 – 11 ions/nm. The measured line width CD is used to convert, the dose-per-nm to a dose-per area, yielding 0.15 – 0.36 ions nm⁻² or 2.3 – 5.8 μC cm⁻². Also, EUV CAR resist of type B was exposed with dense lines-and-spaces patterns using an ASML NXE: 3300B at a dose range between 32 and 50 mJ cm⁻².

Figure 4 shows CD SEM images of lines-and-spaces with 40- and 50-nm pitch (top and center row, respectively) in EUV resist of type A with SHIBL. The trench width increases with ion dose, in a similar fashion for all the three pitches. Therefore the line width (left-bottom panel) decreases with ion dose. The minimum trench width is 14.5 nm, which is marginally larger than the smallest contact hole (see previous section). For 40- and 50-nm pitch a 1:1 pitch was reached. The LWR is shown in the right bottom panel. Minimal LWR is observed at a dose close to 4 ions per nm. The outlier of 5.1-nm (3σ) LWR at 40-nm pitch at 5.2 ions per nm is attributed to pattern collapse (see e.g. top-right panel of Figure 4). Figure 5 shows CD SEM images for 40-nm pitch and graphs of the measured CD and LWR of lines-and-spaces with 40- and 50-nm pitch in EUV resist of type B with EUVL. A minimum of 3.9 nm (3σ) LWR is obtained for the 50-nm pitch lines-and-spaces at a dose of 42-mJ cm⁻².

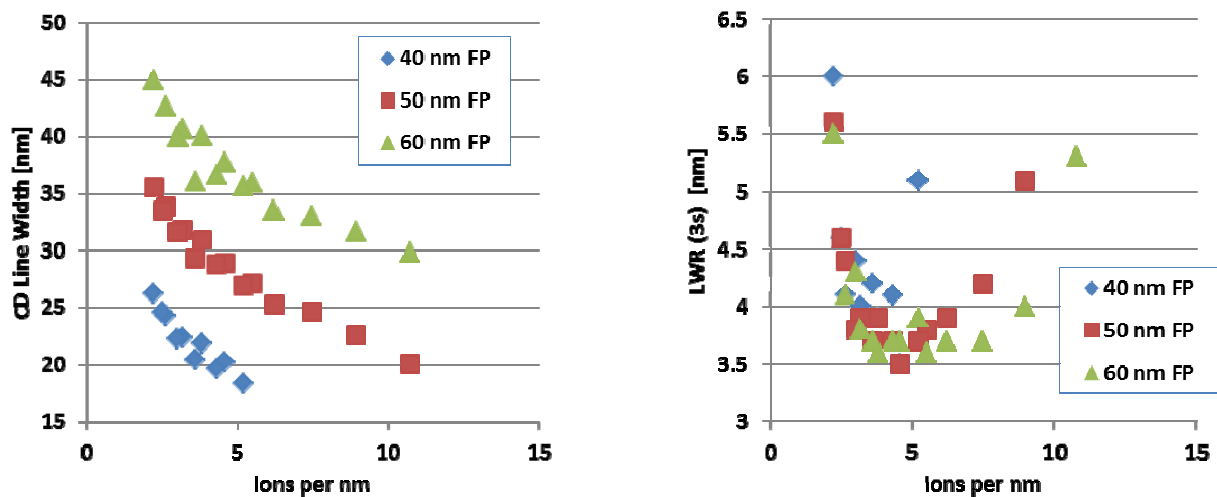
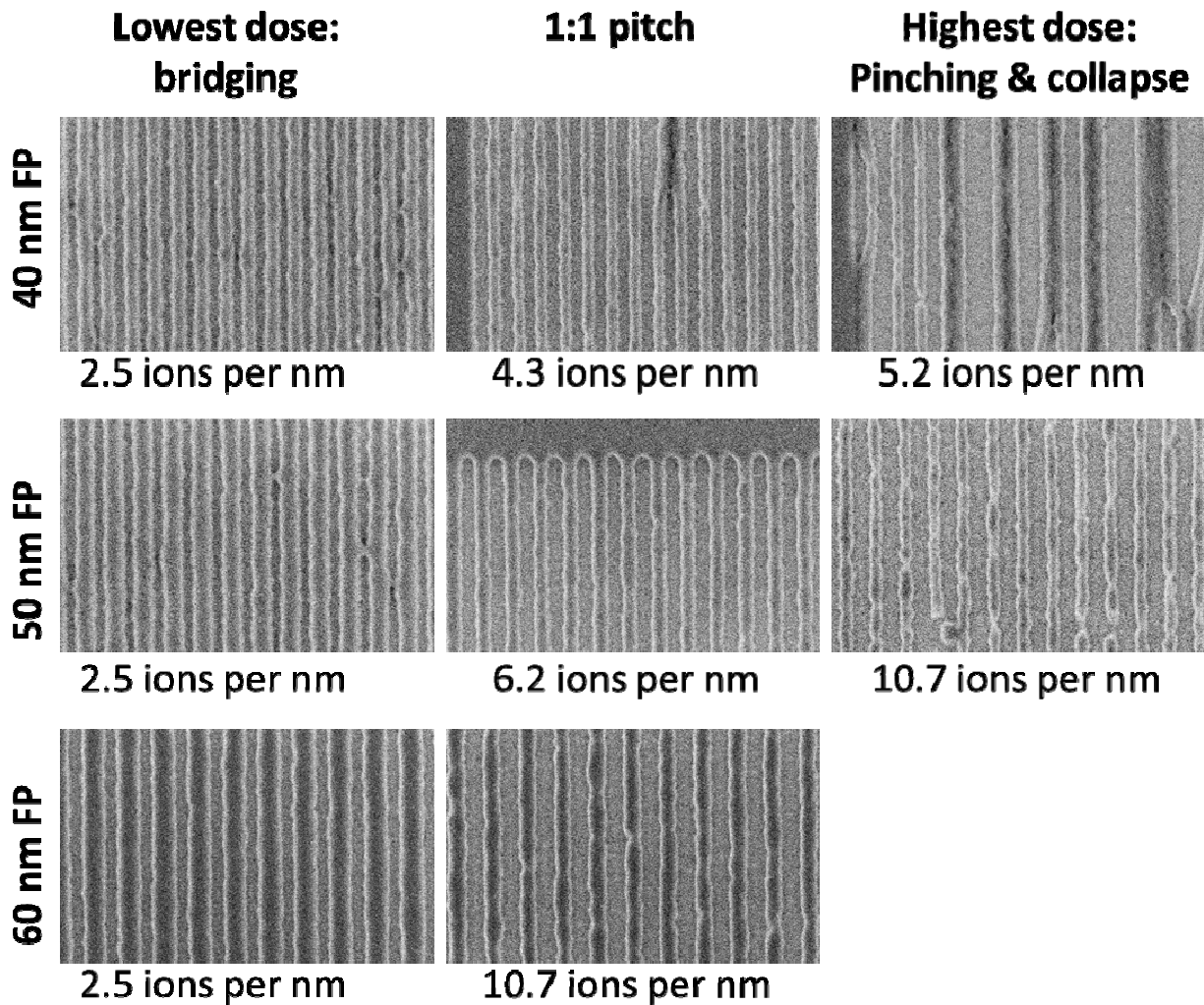


Figure 4 Top respectively center row: CD SEM images of lines-and-spaces at 40- respectively 50-nm pitch in CAR resist A exposed with SHIBL at too low, optimal and too high dose. The bottom row shows the line CD (left panel) and the LWR (right panel) as a function of ion dose.

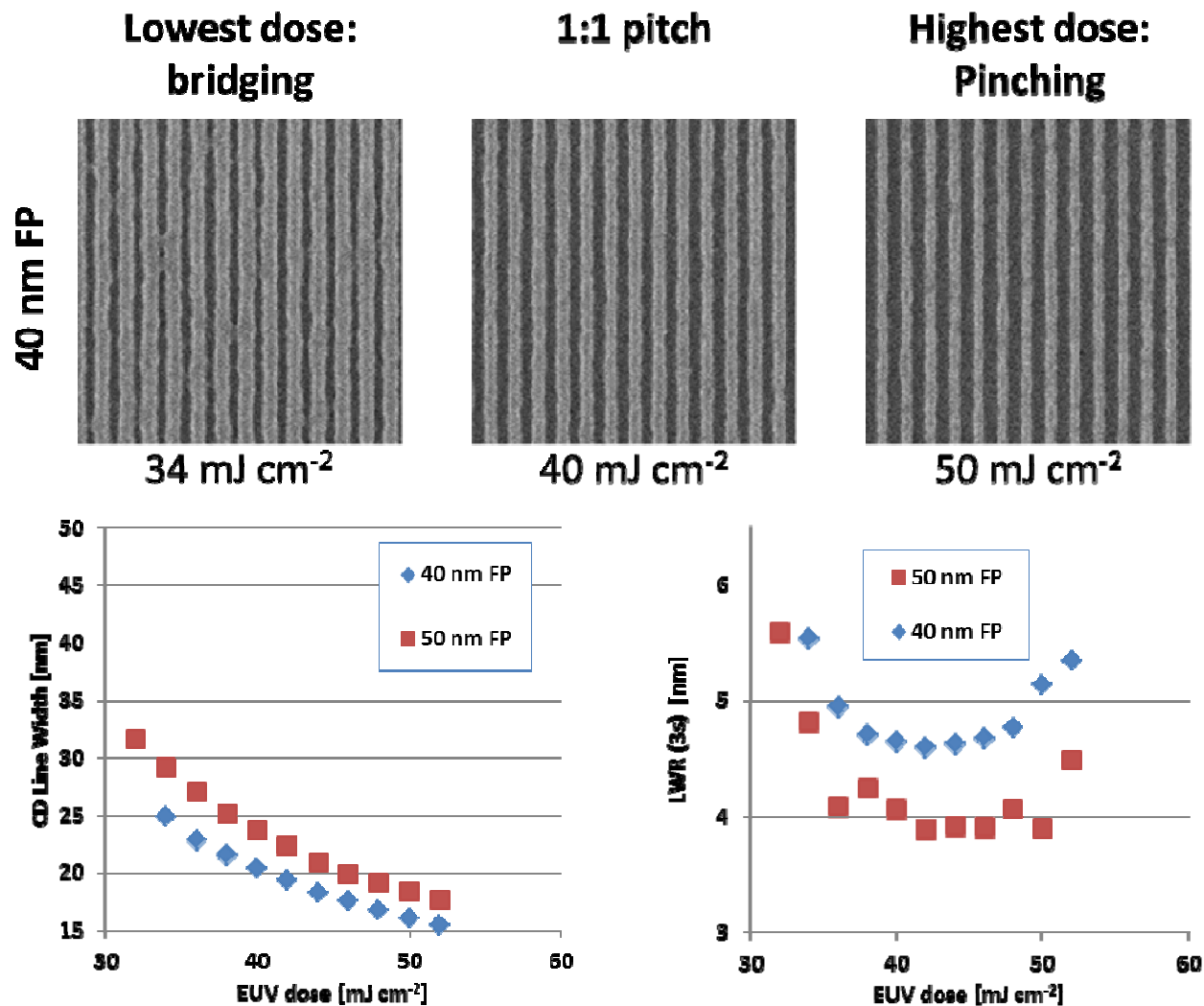


Figure 5 CD SEM images of lines-and-spaces at 40-nm pitch in CAR resist of type B exposed with EUVL at too low, optimal and too high dose. The bottom row shows the line CD (left panel) and the LWR (right panel) as a function of EUV dose, for lines-and-spaces at 40- and 50-nm pitch.

5. DISCUSSION

5.1. CD and LCDU of the contact holes

Visual inspection of the CD SEM images of the SHIBL exposures (Figure 3a-c) shows considerable variations in the contact hole CD, especially at the lowest and the highest doses. There are many holes that are noticeably smaller than average. Nevertheless, the measured CD and LCDU values do not confirm these variations (see Figure 3d). At the lower dose exposures, the CD evaluation software (Hitachi Terminal PC V8) rejected more than 50% of the contact holes because of a minimal-size (closed-contact-hole) criterion and at the higher dose because of a shape criterion (bridging, kissing).

A closer inspection and analysis of the exposure at 87 ions per contact hole (Figure 3a) reveals the following. Many holes are not used by the SW to calculate CD, although visually their shape looks good. The CD evaluation software classifies these holes as closed. Their size is significantly lower than the reported average. This suggests that SHIBL is capable of patterning dense CH at even tighter pitches /CDs, e.g. 30-nm full pitch. It should be noted that the exclusion of smaller holes from the measured population led to an underestimation of the LCDU at these low doses. At 260 ions per hole, a large fraction of the holes is distorted. This effect is currently not understood and under investigation. The

best SHIBL exposures of contact holes are obtained at a dose of 150 ions per contact hole (approximately 10 times the large-area dose-to-clear). At this dose the contact hole array prints at 40-nm pitch with a CD of 17.0 nm and an LCDU of 6.2 nm (3σ). The EUVL exposure of EUV CAR resist of type B (Panel 3e) has a CD of 20.2 nm and an LCDU of 2.9 nm. This LCDU is less than half the value of the SHIBL exposure on EUV CAR resist of type A. Further work with improved SHIBL and CD-SEM protocols are needed to understand the differences.

5.1.1. CD and LWR of lines-and-spaces

Figure 4 shows that in both SHIBL and EUVL there is for each pitch an ion respectively EUV dose that yields a 1:1 ratio of the line-and-spaces CD.

At a full pitch (FP) of 40 nm, the required He^+ ion dose is about 4 ions/nm and at 50 nm, 6.5 ions/nm. In SHIBL, the LWR is largely the same for 40-, 50 and 60-nm pitch, at least for ion doses between 3 and 7 ion per nm. At low He^+ ion dose the trenches are fragmented due to bridging between the lines. At high-dose, the lines collapsed and the lines are pinched. For the 40-nm pitch, the pattern collapse at the highest dose caused an exceptionally high LWR value. In future SHIBL experiments, improved rinsing after development is expected to prevent pattern collapse.

Figure 5 shows that a 1:1 pitch of the lines-and-spaces is reached at an EUV dose of 40- and 38-mJ cm^{-2} for 40- and 50-nm pitch, respectively. Comparison of the CD graphs in Figure 4 and Figure 5 conveys that the dose-dependence of the line- (and hence trench-) width is not completely similar for EUVL and SHIBL. In EUVL, the 40- and 50-nm CD curves (lower-left panel of Figure 5) approach each other at higher EUV dose. Contrarily, in SHIBL (lower-left panel of Figure 4) the difference in CD for different pitches is almost constant for all ion doses. We attribute this to the higher NILS of SHIBL as compared to EUVL.

Furthermore, in EUVL a significantly higher LWR is observed at 40-nm pitch than at 50-nm pitch. In SHIBL, the LWR is almost independent of the pitch, except for too high ion doses (i.e. where pattern collapse starts to occur).

5.1.2. Proximity effect in electron beam and helium ion beam lithography

Because of negligible lateral and/or backward scattering of He^+ ions, proximity effects in SHIBL are non-existing. This is demonstrated at the edges of the dense contact holes arrays of Figure 3a-c: there is no difference visible between the contact holes at the edge and those at the interior of the arrays. For the same reasons, the trench width widening as a function of ion dose in Figure 4 is almost independent of the pitch.

Electron beam lithography, concept-wise similar to SHIBL, is not capable of writing similar dense patterns in EUV CAR resists without extensive proximity effects. Proximity correction is indispensable to counteract the strong contribution to the resist activation by backscattered electrons. The absence of proximity effects is a clear advantage of SHIBL over EBL, although today EBL is often used to pre-screen EUV resist.

5.1.3. Outlook

In this paper, we introduced SHIBL as a possible novel method for the (pre-)screening of EUV resists on fundamental properties. Since no mask is required, one can quickly evaluate the printability of more complex patterns.

The direct low-energy SE generation by the primary particles in SHIBL might improve pattern resolution at the cost of uniformity. Hence, SHIBL experiments may provide data for the study of pattern resolution blurring due to SE diffusion. Further research aiming at understanding the interaction cascade for the resist activation is planned and is expected to yield insights in the resist activation mechanism. With that knowledge hopefully better resist can be developed.

6. CONCLUSIONS

In this paper we have shown that CAR EUV resist can be exposed with scanning helium ion beam lithography, yielding feature sizes below 20 nm.

The holes and trenches made with SHIBL are alike exposures with EUVL. However, the obtained pattern uniformity in terms of LCDU and LWR is worse for SHIBL compared to EUVL. Further work in optimization of the experimental conditions of SHIBL and CAR resist processing are ongoing; it is expected that better uniformity results can be obtained. The presented SHIBL experiments support the concept that resist activation by 30-keV He^+ ions is similar to that in EUVL. Hence, SHIBL is a potential economically attractive technology for EUV resist screening on sensitivity, resolution and pattern uniformity. Furthermore, contrary to electron beam lithography, resist activation mainly occurs through the directly generated low-energy secondary electrons. However, more research on the (dis)similarities between EUVL and SHIBL is still needed.

Advantages of SHIBL are the high yield of low-energy SEs per ion and the ultra-local interaction of helium ions with target atoms. The former explains the good imaging qualities. The latter leads to ultra-low proximity effects and therefore an accurate projection of the (arbitrary) pattern on the resist.

7. ACKNOWLEDGEMENT

This research is supported by the Dutch Technology Foundation STW, which is part of the Netherlands Organization for Scientific Research (NWO), and which is partly funded by the Ministry of Economic Affairs. We gratefully acknowledge Renée Pohlmann (TNO) for project management.

REFERENCES

- [1] Gallatin, G.M., "Resist blur and line edge roughness," Proc. SPIE 5754, 38-52 (2005).
- [2] Ayothi, R., Singh, L., Hishiro, Y., Pitera, J.W., Sundberg, L.K., Sanchez, M.I., Bozano, L., Virwani, K., Truong, H.D., Arellano, N., Petrillo, K., Wallraff, G.M., Hinsberg, W.D. and Hua, Y., "Fundamental study of extreme UV resist line edge roughness: Characterization, experiment, and modeling," J. Vac. Sci. Technol. B 30 06F506 (2012).
- [3] Thackeray, J., Cameron, J., Jain, V., LaBeaume, P., Coley, S., Ongayi, O., Wagner, M., Rachford A. and Biafore, J., "Pursuit of lower Critical Dimensional Uniformity in EUV resists," J. Photopolym. Sci. Technol. 26, 605-610 (2013).
- [4] Sidorkin, V., van Veldhoven, E. van der Drift, E., Alkemade, P., Salemink, H. and Maas, D., "Sub-10-nm nanolithography with a scanning helium beam," J. Vac. Sci. Technol. B 27, L18 (2009).
- [5] Maas, D.J., van der Drift, E.W., van Veldhoven, E., Meessen, J., Rudneva, M. and Alkemade, P.F.A., "Nano-engineering with a focused helium ion beam," Mater. Res. Soc. Symp. Proc. 1354, 33-46 (2011).
- [6] van der Drift, E.W.J.M. and Maas, D.J. "Helium ion lithography," in M. Stepanova & S Dew (Eds.), [Nanofabrication, techniques and principles], Springer, 93-116 (2010).
- [7] Bozano, L.D., Brock, P.J., Truong, H.D., Sanchez, M.I., Wallraff, G.M., Hinsberg, W.D., Allen, R.D., Fujiwara, M. and Maeda, K. "Bound PAG resists: An EUV and electron beam lithography performance comparison of fluoropolymers," Proc. SPIE 7972, 797218 (2011).
- [8] Ekinci, Y., Vockenhuber, M., Terhalle, B., Hojeij, M., Wang, L. and Younkin, T.R. "Evaluation of resist performance with EUV interference lithography for sub-22 nm patterning," Proc. SPIE 8322, 83220W (2012)
- [9] Li, W.-D., Wu, W. and Williams, R.S. "Combined helium ion beam and nanoimprint lithography attains 4nm half-pitch dense patterns," J. Vac. Sci. Technol. B 30 06F304 (2012).
- [10] Hill, R. and Rahman, F.H.M. "Advances in helium ion microscopy," Nucl. Instrum. Methods A 645, 96-101 (2011)
- [11] Kozawa T. and Tagawa, S. "Radiation Chemistry in Chemically Amplified Resists," Japanese Journal of Applied Physics 49, 030001 (2010).
- [12] Torok, J., del Re, R., Herbol, H., Das, S., Bocharova, I., Paolucci, A., Ocola, L., Ventrice Jr., C., Lifshin, E., Denbeaux, G. and Brainard, R. "Secondary electrons in EUV lithography," J. Photopolym. Sci. Technol. 26, 625-634 (2013).
- [13] Petrov, Y. and Vyvenko, O. "Secondary electron emission spectra and energy selective imaging in helium ion microscope," Proc. SPIE 8036, 80360O (2011).
- [14] Henke, B.L., Gullikson, E.M. and Davis, J.C. "X-ray interactions: photoabsorption, scattering, transmission, and reflection at E=50-30000 eV, Z=1-92," [Atomic Data and Nuclear Data Tables] Vol. 54 (no.2), 181-342 (July 1993). (http://henke.lbl.gov/optical_constants/).
- [15] Fedynyshyn, T.H., Goodman, R.B., Cabral, A., Tarrío, C. and, Lucatorto, T.B. "Polymer photochemistry at the EUV wavelength, Proc. SPIE, 7639, 76390A (2010).
- [16] Ziegler, J.F., Ziegler, M.D. and Biersack, J.P. "SRIM – The stopping and range of ions in matter," Nucl. Instr. Methods B, 268, 1818-1823 (2010).
- [17] Winston, D., Ferrera, J., Battistella, L., Vladár, A.E. and Berggren, K.K., "Modeling the point-spread function in helium-ion lithography," Scanning, 34 121-128 (2012).
- [18] Brodie, A., Kojima, S., McCord, M., Grella, L., Gubiotti, T., and Bevis, C. "Preliminary investigation of shot noise, dose, and focus latitude for E-Beam Direct Write," Proc. SPIE 8680, 868029 (2013).